How Severe Acute Respiratory Syndrome Coronavirus-2 Aerosol Propagate through the Age-Specific Upper Airways?

Mohammad S. Islam [1*], Puchanee Larpruenrudee[1], Suvash C. Saha[1*], Oveis Pourmehran[2], Akshoy Ranjan Paul[3], Tevfik Gemci[4], Richard Collins[5], Gunther Paul[6], and Yuantong Gu[7]

[1] School of Mechanical and Mechatronic Engineering, University of Technology Sydney (UTS), 15 Broadway, Ultimo, NSW-2007, Australia
[2] Adelaide Medical School, The University of Adelaide, SA 5005, Australia
[3] Department of Applied Mechanics, Motilal Nehru National Institute of Technology Allahabad, Prayagraj-211004, Uttar Pradesh, India.
[4] Braun Medical, Irvine, CA 92614, USA
[5] Biomechanics International, Cranberry Township, PA 16066, USA
[6] James Cook University, Australian Institute of Tropical Health and Medicine, Townsville, QLD 4810, Australia
[7] School of Mechanical, Medical and Process Engineering, Faculty of Engineering, Queensland University of Technology, Brisbane-4000, Australia.

Corresponding authors: mohammadsaidul.islam@uts.edu.au, Suvash.Saha@uts.edu.au

Abstract

The recent outbreak of the COVID-19 causes significant respirational health problems, including high mortality rates worldwide. The deadly corona virus-containing aerosol exposes to the atmospheric air through sneezing, exhalation or talking, assembling with the particulate matter, and subsequently transferring to the respiratory system. The recent outbreak illustrates that the severe acute respiratory syndrome (SARS) Coronavirus-2 is deadlier for aged people than for other age groups. It is evident that the airway diameter reduces with age, and an accurate understanding of the SARS aerosol transport through different elderly people's airways could potentially help the overall respiratory health assessment, which is currently lacking in the literature. This first-ever study investigates the SARS covid-2 aerosol transport in age-specific airway systems. A highly asymmetric age-specific airway model and Fluent solver (Ansys 19.2) are used for the investigation. The computational Fluid Dynamics (CFD) measurement predicts higher SARS Covid-2 aerosol concentration to the airway wall for older adults than for younger people. The numerical study reports that the smaller SARS Coronavirus-2 aerosol deposition rate in the right lung is higher than in the left lung, and the opposite scenario occurs for the larger SARS Coronavirus-2 aerosol rate. The numerical results report a fluctuating trend of pressure at different generations of the age-specific model. The findings of this study would improve the knowledge of the SARS Coronavirus-2 aerosol transportation to the upper airways which would thus ameliorate the targeted aerosol drug delivery system.

Keyword: SARS Coronavirus-2 Aerosol, Aging, Respiratory Health, Targeted Drug Delivery, CFD

1. Introduction:

The outbreak of SARS Coronavirus-2, commonly known as Covid-19 has, in late 2019, posed different challenges to different socio-demographic groups. The disease has hit the elder population harder than any other age groups because of the latter's pre-existing co-morbidities;

viz. hypertension, diabetes, cardiovascular diseases, chronic pulmonary and even renal diseases etc. (Al-Zahrani, 2021; Smorenberg *et al.*, 2021). Aging changes respiratory physiology, pathology and their working, more often irreversibly, posing a serious concern especially during pulmonary infection. Subsequently, it affects the sensitivity and survivability of the aged patients, eventually make them more vulnerable to Covid-19 (Lowery, 2013; Miller and Linge, 2017; Liu et al., 2020). More than 95% of the Covid-19 deaths considered in this study included populations over 60 years of age, while more than 50% of the death included people over 80 years of age as revealed in a WHO data (Sandoiu, 2021). Due to many degenerative processes taking place in the body, vital capacity (i.e. total amount of air exhaled after maximal inhalation) of the lungs of the aged people are decreased and hence, it requires excess work to maintain normal breathing (Stocks and Quanjer, 1995).

Researchers investigated the relation of aging with the severity of Covid-19 for patients located in Australia (Holt *et al*., 2020), Israel (Clarfield and Jotkowitz, 2020), China (Guo *et al*., 2020), India (Singh *et al*., 2020) and in many other countries (Ayoub *et al.,* 2020; Davies *et al*., 2020). It is found that the fatality rate of Covid-19 patients in countries like Italy, Spain, China which were severely affected bySARS Coronavirus-2 pandemic in its first outbreak, increased exponentially with age of the patients (Santesmasses *et al.*, 2021). Possible remedies were also suggested by some researchers (Koff and Williams, 2020; Perrotta *et al*., 2020; Mueller *et al*., 2020) for elderly patients, which include those in long-stay residential care home and hospitals. Amongst all, the SARS viruses, their SARS Coronavirus-2 variants can reach the lower airways, causing severe damage to pulmonary tissues, thus turning them from spongy to stiffer (fibrosis and scarring) forms, subsequently resulting in high fatality from pneumonia (Zhu *et al.,* 2020). A recent study by Edwards *et al*. (2021) suggests that the formation of droplets from the mucus lining of the human airways and aerosol exhalation increase with acute Covid-19 infection and patients' body mass index (BMI) multiplied with increased age. The susceptibility to disintegrated mucus layers in the airway lining is much higher in aged populations, making the aged patients a super-spreader. Aging is an irreversible and degenerative phenomenon. Various physiological and immunological factors responsible for aging of the human respiratory system are discussed by the researchers (Rossi*et al*., 1996; Pride, 2005 and Shama and Goodwin, 2006). Aging of human airways is reflected in the changes of material (elasticity) and anatomical (lumen diameter and wall thickness) properties because of morphological and tissue variations (Lai-Fook and Hyatt, 2000). The diameter of the smaller airways (bronchioles <2 mm) becomes narrow with age for people aged over 40 years and a 10% reduction in bronchioles is seen for people aged between 50 and 80 years (Niewoehner and Kleinerman, 1974). The lungs are never fully empty and the amount of air volume left after complete expiration is termed residual volume (RV). With age, the residual volume increases, mainly due to the reduction in airway diameters (Leblanc, 1970). The forced vital volume (FVC) for an expiration during a spirometry test is found to be reduced by 50% due to intrinsic reduction in the mean diameter of the membranous bronchioles (Knudson, 1991). The airway walls are thickened due to increase of collagen and membranes (Montaudon *et al*., 2007) in the lungs of older people suffering from severe asthma (Bai *et al*., 2000). Hence elderly patients with history of respiratory illness are more vulnerable to Covid-19 infection. Changes due to aging (compliance of lung and mechanical properties of airways) (Kim *et al.,* 2017) increase the chances of lung injury during mechanically ventilated procedures.

Respiratory routes are preferred for administering drugs for both pulmonary as well systematic diseases (Jaafar-Maalej *et al*., 2009). Adapting the morphological properties of lungs into the respiratory tract models, selection of ventilation parameters (breathing patterns etc.), aerosol characteristics (size, shape, material properties), growth of obstacles (lesions/tumours) in the airways, fluid-wall interactions and in the in-vitro studies are essential in predicting the

performance of aerosol transport (Thompson, 1998; Labiris and Dolovich, 2003; Srivastav *et al.*, 2019a; Shukla *et al.*, 2020; Singh *et al.*, 2021). Various researchers (Srivastav *et al*., 2013; Srivastav *et al*., 2014; Islam *et al.*, 2017; Islam *et al.,* 2018) investigated the particle and aerosol transport to human airways, providing insight into the absorption and deposition mechanisms of inhaled drugs with a view of designing better drugs for targeted drug delivery through pulmonary routes. Many researchers (Kim *et al*., 2015; Das *et al*., 2018; Ostrovski *et al*., 2019; Tiwari *et al.*, 2021) focussed on targeted delivery into the lungs using experimental as well as CFD methods to study the aerosol transport dynamics leading to development of better inhalation devices. Recently, Islam *et al.* (2020) reviewed the efficacy of various numerical models available to estimate deposition of aerosols in the human airways.

Amidst the outbreak of Covid-19, the focus has now shifted to investigation of the transmission of SARS Coronavirus-2 viruses in the form of aerosols and droplets in the public places and to the respiratory tract. A plethora of researches is conducted in recent times to study the transmission behaviour of SARS Coronavirus-2 in various public places, like elevators (Dbouk and Drikakis, 2021), escalators (Li et al., 2021a), dental clinic (Li et al., 2021b), hospital isolation rooms (Bhattacharyya et al., 2020), vehicle parking areas (Nazari et al., 2021), buses (Zhang et al., 2021), passenger aircraft (Talaat et al., 2021), classrooms (Foster and Kinzel, 2021), restaurants and cafeterias (Liu et al., 2021, Wu et al., 2021), conference rooms (Mirikar et al., 2021), classrooms (He et al., 2021), public restrooms (Schreck et al., 2021), in a city (Zheng et al., 2021) and even during face-to-face scenario with utterance (Ishii et al., 2021). On the other hand, Jarvis (2020) found that the SARS Coronavirus-2 borne aerosol particles can combine with particulate matter (PM) present in the atmosphere, possibly leading to even higher infection rates. The habitual ciggarette smokers also face higher risks of toxic particle deposition in the distal regions of the respiratory tract (Paul et al., 2021). Tang *et al*. (2020) and Mutuku *et al*. (2020) confirmed that the plausibility of aerosol transmission for SARS Coronavirus-2 viruses is very high. Hence, suitable strategies are discussed by the researchers to contain or minimise airborne transmission of atmospheric viral loads through ventilation (Jarvis, 2020) such as in hospitals and isolation rooms (Bhattacharyya *et al.,* 2020). Human nasal passages can be of 5-10 μm in lumen. The airways are, however reduced to 2.5-5 μm in the trachea and to 0.1-2.5 μm in further downstream locations. Guzman (2020) revealed that the size of the particles laden with SARS Coronavirus-2 RNA can be as small as 0.25-1 μm, which can often be readily inhaled into the respiratory tract and could easily be transmitted airborne by diffusion. On the other hand, larger particles containing viral loads (2.5-10 μm) have a chance to deposit in the nasal, oro-pharyngeal, laryngeal and tracheal regions of the respiratory system due to gravitational settling and cause infection. Mallik *et al.* (2020) conducted experimentation to study the aerosol transport in bronchioles and found that the aerosol deposition increases with bronchiole diameter. It was also pointed out that a high breath-hold time can increase the possibility of viral infection, especially in a crowded place as it promotes further aerosol deposition in the alveoli.

It is evident that airway diameter reduces with age and a precise understanding of the SARS Coronavirus-2 aerosol transport through pulmonary airways of different elderly people airway could potentially help improve the overall respiratory health assessment which is lacking in the literature. The present study aims to numerically investigate the SARS Coronavirus-2 aerosol transportation to age-specific airway system for the first time.

2. Numerical Methods

The study considered steady laminar flow and analysed the SARS coronavirus-2 aerosol transportation to the upper airways of an age-specific lung. Ansys-Fluent (v.19.2) solver and Lagrangian approach are employed to solve the fluid flow and particle transport equations. The study solved the steady mass and momentum equations;

$$\nabla.(\rho\vec{v}) = 0 \tag{1}$$

$$\nabla.(\rho\vec{v}\vec{v}) = -\nabla p + \nabla.(\mu(\nabla\vec{v} + \nabla\vec{v}^{T})) + \rho\vec{g} \tag{2}$$

where, $\rho\vec{g}$ and p denote gravitational body force and static pressure, respectively. The molecular viscosity is defined as μ.

The numerical study solved the internal energy equation for Brownian motion of the nano-size SARS Coronavirus-2 aerosol

$$\nabla\cdot\left(\rho\vec{v}e\right) = -\nabla\cdot\vec{J} \tag{3}$$

where specific internal energy is e and $\vec{J}$ is the heat flux.

The inhalation condition at the mouth-throat region is highly complex, and there is no established velocity profile for the inhalation. Studies to date mostly used uniform inlet conditions for one-way inhalation (Islam *et al*., 2021b; Kuprat, 2021; Zhao *et al.*, 2021), and parabolic (Bass *et al*., 2021; Chen *et al*., 2021; Fan *et al., 2021;* Hayati *et al*., 2021*)*. During inhalation, the uniform flow field could become highly turbulent at the mouth-throat area at flow rate >30 lpm (Islam *et al.*, 2018; Islam *et al.*, 2019; Kleinstreuer *et al*., 2003; Zhang *et al.*, 2005), and the flow profile becomes parabolic at the trachea and upper airways (Gemci *et al*., 2008; Islam *et al*., 2017a). This study used uniform inlet conditions at the mouth-throat inlet. The overall SARS Coronavirus-2 aerosol transportation to the mouth and upper airways is analysed for the flow rates of 7.5 lpm and 15 lpm. The outlet condition at the truncated outlets are pressure-based, and zero pressure is assigned at the end of the branches. This study did not consider all the bifurcations; only the first 5-bifurcations were considered in the analysis. Therefore, the open outlet condition used at the outlet which is adopted from the published literature (Cui *et al*., 2021; Islam *et al*., 2021a).

The scatter in the particulate size of SARS Coronavirus-2istiny, and in the isolated condition, the size is about 120 nm (https://www.pptaglobal.org/media-and-information/ppta-statements/1055-2019-novel-coronavirus-2019-ncov-and-plasma-protein-therapies).
However, a recent study shows the virus size could vary, and it could be up to 1000nm (Liu *et al*., 2020). The isolated SARS Coronavirus-2 viruses could aggregate or transport as droplets during exhalation, coughing or sneezing. Therefore, the overall diameters of the virus-laden aerosol will increase, which is evident in the literature (Chirizzi *et al*., 2021). This study used three different sized (120nm, 500nm and 1µm) SARS Coronavirus-2 aerosols and analysed the deposition at the upper bronchioles for aged lungs.

Therefore, the particle transport equations include Brownian motion for the nano-size SARS Coronavirus-2 aerosol (Inthavong *et al.*, 2009; Islam *et al.*, 2021c).

$$\frac{du_i^p}{dt} = F_D + F_{Brownian} + F_{Lift} + \frac{\rho_p - \rho_g}{\rho_p} g_i$$

$$F_D = \frac{1}{C_c} C_D A_p \frac{\rho_g \left|u_i^g - u_i^p\right| (u_i^g - u_i^p)}{2m_p} = \frac{18\mu_g}{\rho_p d_p^2 C_c} (u_i^g - u_i^p) \quad (4)$$

$$C_c = 1 + \frac{2\lambda}{d_p}(1.257 + 0.4e^{\frac{-0.11 d_p}{2\lambda}})$$

where F_D is the force due to drag, drag coefficient is C_D, A_p is the aerosol area, and C_c is the Cunningham factor. The C_c value for 120nm, 500nm and 1 µm aerosols are 2.52, 1.39 and 1.19 respectively. λ is gas molecules mean free path. ρ_p is the aerosol density and ρ_g is the air density, respectively. g_i is gravitational term. μ_g denotes gasviscosity and d_p is aerosol diameter. For the low Reynolds number of the particle ($\mathrm{Re}_p < 0.5$), the drag coefficient C_D is defined as (Haider *et al.*, 1989);

$$C_D = \frac{24}{Re_p}, \quad Re_p < 0.5 \quad (5)$$

where the particle Reynolds number;

$$Re_p = \rho_g \frac{d_p |u_r|}{\mu_g} \quad (6)$$

where, u_r is the relative velocity. The Brownian force amplitude is;

$$F_{Brownian} = \zeta \sqrt{\frac{\pi S_0}{\Delta t}} \quad (7)$$

where ζ is the unit Gaussian random number variance, Δt is time-step integration of the aerosol. The spectral intensity (S_0) is defined as

$$S_o = \frac{216\mu k_B T}{\pi^2 \rho_p d_p{}^5 (\frac{\rho_p}{\rho_g})^2 C_c} \quad (8)$$

T is the absolute temperature of the gas, k_B is defined as Boltzmann constant, ρ_g is the air density.

The numerical study used SIMPLE scheme for the pressure and velocity coupling. Second order discretisation technique is employed for the energy and momentum equations (Kumar *et al.*, 2019). The SARS Coronavirus-2 aerosol particles are considered spherical (https://www.nih.gov/news-events/nih-research-matters/novel-coronavirus-structure-reveals-targets-vaccines-treatments). The available literature (Goldsmith *et al*., 2020) reports that SARS Coronavirus-2 aerosol particles are spherical and consist of dark dots on the spherical shape. Therefore, spherical SARS Coronavirus-2 aerosols are used for the analysis and the density used is 1.0 g/cm^3 (Islam et al., 2021c). The SARS Coronavirus-2 aerosols are injected from the mouth-throat inlet, and all aerosols are inserted only once. The SARS Coronavirus-2 aerosol distribution is uniform as the velocity, and mono-disperse aerosols are injected. The number of particles convergence also tested for various sets of particles, and a total of 13460 particles was injected from the inlet face for the final analysis. The interaction between air and the SARS Coronavirus-2 aerosols is considered. The residual convergence criterion for the continuity equation is 0.0001 (10^{-4}), and for the energy equation is 0.000001 (10^{-6}) in this study. The hybrid initialisation technique is used for the numerical simulation.

The SARS Coronavirus-2 aerosol deposition condition at the airway wall is used as 'trap' (Ghosh et Al., 2020, Islam et al., 2019), which means, during inhalation, if the particle touches the airway wall, the system will count it as deposited. The velocity of the SARS Coronavirus-2 aerosol particles will be zero at the airway wall as the wall is considered static, and the aerosol trajectory will terminate at the wall. The deposition efficiency (DE) of the SARS coronavirus-2 aerosol is based on the ratio of the trapped aerosol and total injected aerosol.

3. Geometrical Development

In the present study,three anatomical models were constructed for 50, 60 and 70-year-old people. The anatomical models in this study contain computed tomography (CT)-Scan based mouth-throat and Weibel's based (Weibel et al., 1963) reconstructed tracheobronchial airway (from the trachea to the first-fifth generations). AMIRA and Geomagic software are used to visualise the CT-Dicom images and 3-dimensional anatomical models are developed. For the tracheobronchial airways, SolidWorks software is used. An earlier study analysed the morphology of the human lung due to aging and reports 10% reduction in the airway size (Niewoehner *et al.* 1974). Later, an analytical equation was developed by Xu and Yu (1986) for the age-specific lung upon the findings of Niewoehner *et al*. (1974). Recently, a computational study analysed the airflow in an age-specific lung and reduced the airway dimension by 10% for people over 50 years (Kim *et al.* 2017). The airway dimension, shape and branching pattern could vary from person to person, depending on age. This study used the data available in the literature along with a 10% reduction for people over 50 years. However, in reality, the airway dimension could be different for various ages people depending on age, sex and other physiological conditions. **Figure 1** shows the reconstructed airway model for the 50-year old lung. For the 60-year and 70-year old models, airway dimensions are reduced by 10%.

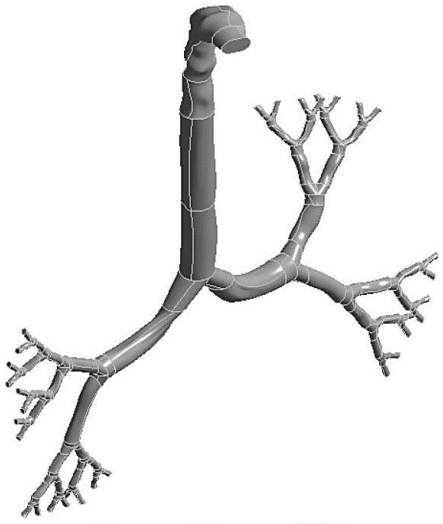

Figure 1. Reconstruction airway model for the lung of a 50-year-old subject.

4. Mesh Generation, Mesh Refinement and Validation

The Ansys meshing module is employed for the computational mesh, and unstructured tetrahedral mesh elements are generated for the three different lung models. The inflation layer is generated adjacent to the airway wall, and the bifurcation area consists of highly dense mesh elements (Srivastav *et al.*, 2019b). Figure 2(a) presents the mesh at the mouth region, and Figure 2(b) presents the mesh element at the first bifurcation area for the 50-year old model. Figures 2(c, d) show the inflation layer mesh at the mouth and outlet region of the lung model. A detailed grid refinement is performed and figure 3 shows the grid convergence results. The final computational model for the 50-year old lung model consists of 2.5 million cells, while the 60-year and 70-year old models consist of 2 million and 1.7 million cells, respectively. The aged model provides the steady solution for the lower number of cells as the airway diameter is reduced.

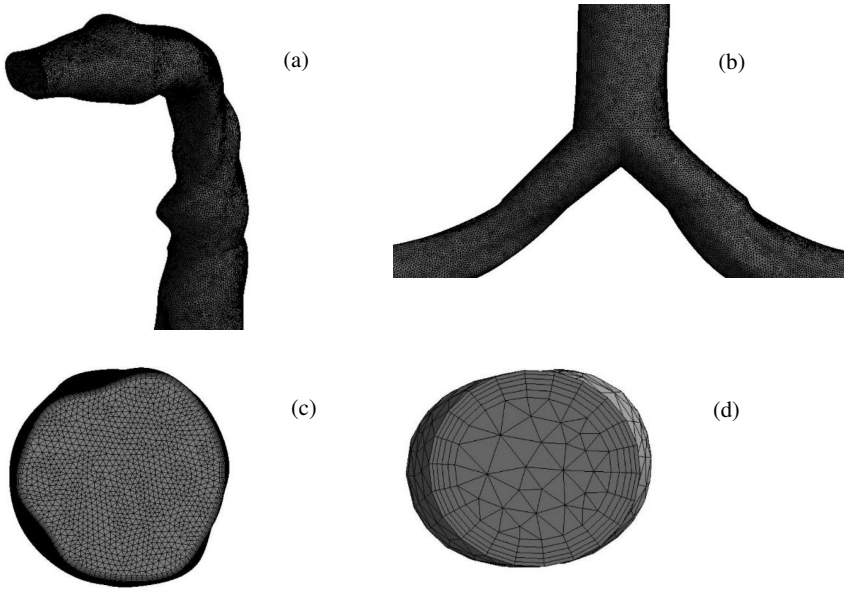

Figure 2. Computational mesh for the airway; **(a)** mouth-throat section, **(b)** first bifurcation, **(c)**inflation mesh at mouth area, and **(d)** inflation mesh at the outlet.

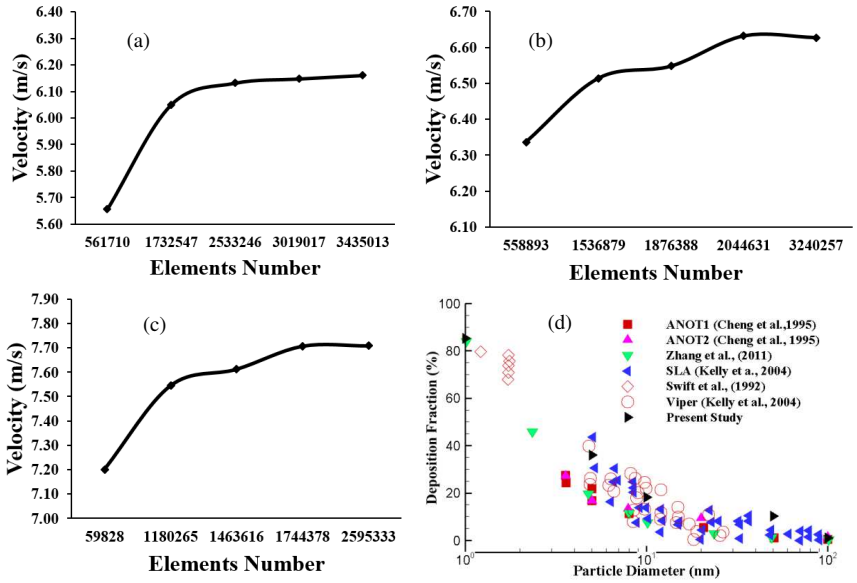

Figure 3. Grid refinement results for (a) 50-year old, (b) 60-year old, (c) 70-year old and (d) deposition fraction comparison with the available literature at 10 lpm flow rate(Cheng *et al.*, 1995a; Cheng *et al*., 1995b; Kelly et al., 2004; Swift *et al*., 1992; Zhang and Kleinstreuer, 2011).

The CFD model is authenticated with the available experimental and computational measurements. The deposition fraction at the upper airway is compared with the available literature findings (Cheng *et al*., 1995a; Cheng *et al*., 1995b; Kelly *et al*., 2004; Swift *et al.*, 1992; Zhang and Kleinstreuer, 2011). The present study used a 50-year old model for the deposition fraction comparison. The present computational results closely align with the published measurement, which eventually supports the present computational study results.

5. Result and Discussion

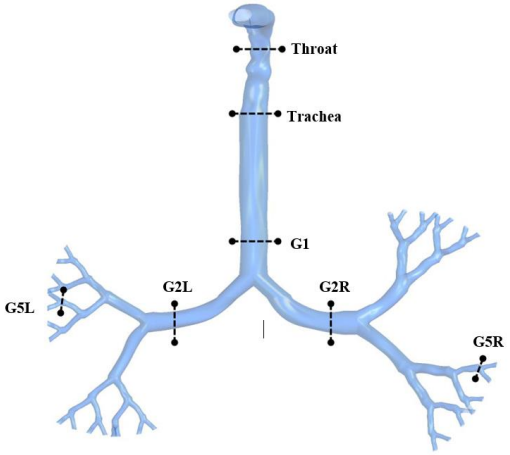

Figure 4. Selected planes for velocity contours at various branches.

Figure 5 presents the velocity contours at selected locations (see Figure 4) of the upper airways from the mouth-throat area to the fifth generation. These contours represent the velocity fields and velocity vectors at 15 lpm inlet condition. Figure 5 (a-c) show the contours for 50-year, 60-year, and 70-year olds, respectively. For 50-year-olds, more complex flows with two vortices are found at the throat, trachea, and generation 1. However, the rest contours show that only one vortex has been formed for both sides of pulmonary generations 2 and the left side of generation 1. Moreover, it can be observed from the figure that no vortex is generated for the right lung in generation 5. For 60-year-olds, the throat and tracheal areas have more complex flows with two vortices. There is only one vortex solution at generation 1 and the left lung at generation 2. For 70-year-olds, the throat and the right lung at generation 2 generate more complex flows with two vortices following by the one vortex solution at the trachea. In terms of the velocity magnitude, the highest velocity is located at the throat area for all three cases. For 50-year-olds, the velocity decreases continuously along with the airway generations. For 60-year-olds, the velocity becomes higher at the left lung of generation 2 and decreases along with the generations. For 70-year-olds, the velocity decreases from the throat area to generation 1 and then increases at the left lung of generation 2 and the right lung of generation 5. The overall velocity and vector contours indicate that the 50-year-old case consists of different flow behaviour for most generations compared to the other two cases. However, the 70-year-old case has higher velocity magnitudes from generation 1 to lower generation than 1. In terms of velocity patterns, only the throat and trachea have similar flow fields in all downstream generations.

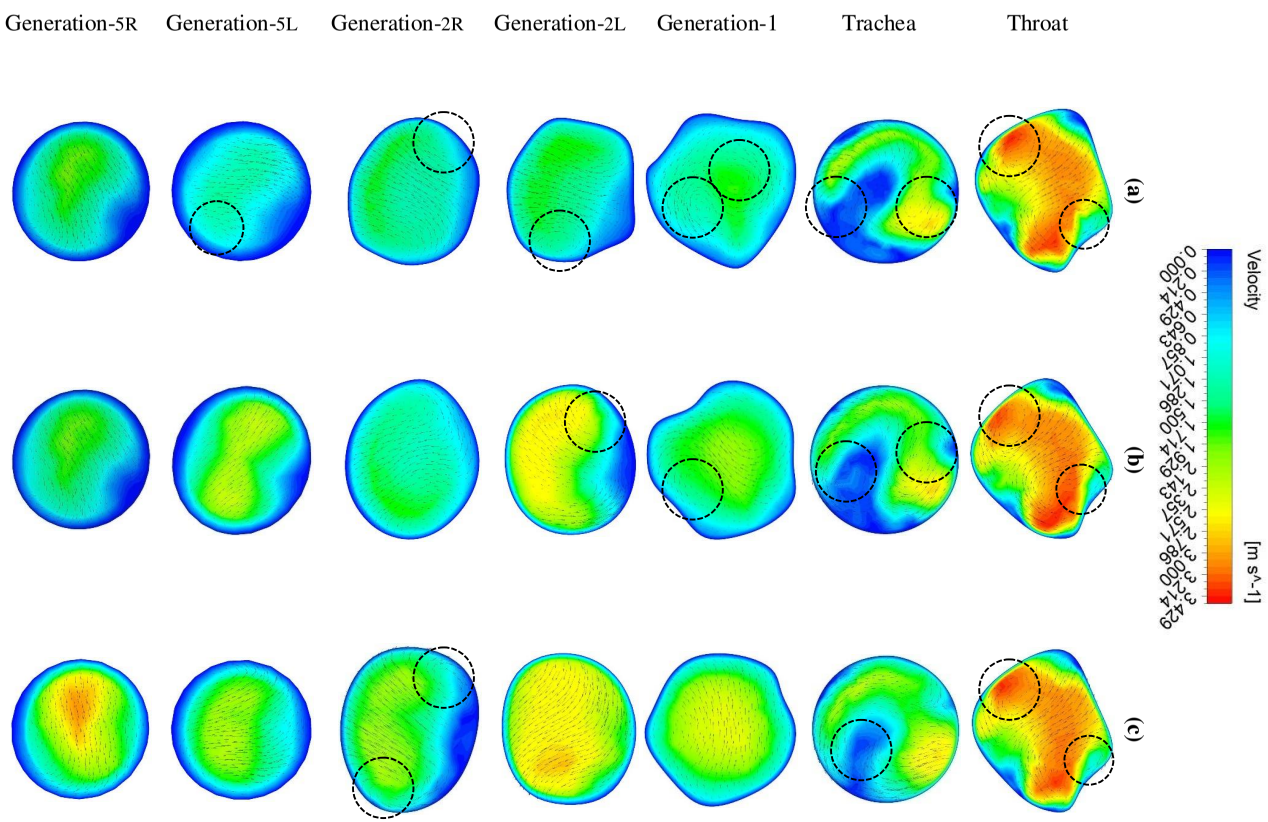

Figure 5. Velocity contours at various positions of the pulmonary models at 15 lpm for **(a)** 50-years old subject, **(b)** 60-years old subject, and **(c)** 70-years old subject.

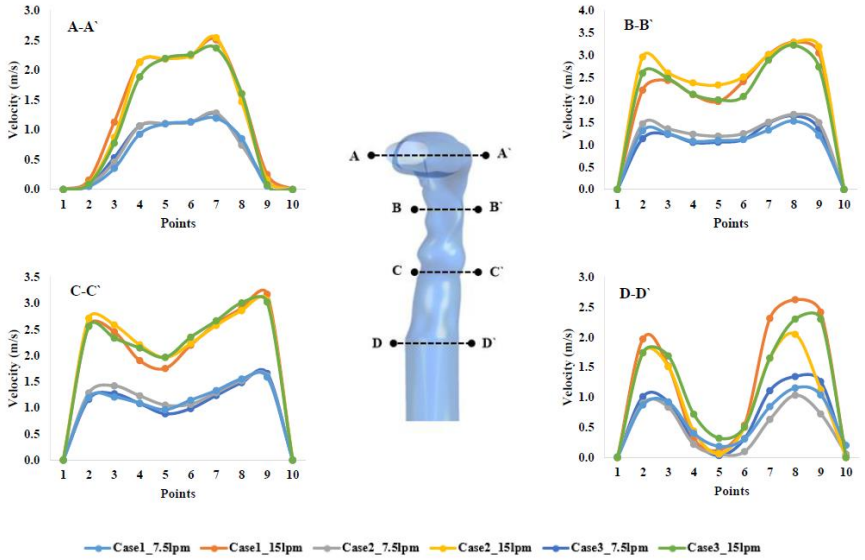

Figure 6. Velocity profiles at various position of mouth area for three lung models with different flow rates. Case 1: 50-years; Case 2: 60-years; Case 3: 70-years old subject.

Figure 6 (a-d) represent the velocity profile across a straight line at different cross-sections along the throat to trachea. According to Figure 6(a-d), the velocity profiles for different cases at lines A, B, C and D reports that the velocity magnitude increase with the flow rate in the central area of the related lines. However, the flow profile across lines A, B, C and D are not identical. Figure 6 (a-d) shows that the velocity magnitude in the proximity to the centerline of the airway decreases from throat to trachea. This behaviour of velocity magnitude stems from the presence of the secondary flow, which is generated due to the bending airways at the throat. Figure 6(d) shows that the velocity in the centre of the trachea is less than 0.5 m/s, which is much lower than other non-central areas. Hence, it can be implied that the airflow in the upper airways passes the out-of-central area of the airway dominantly. Therefore, it is anticipated that the SARS coronavirus aerosol deposition on the wall of the trachea decreases since the velocity is high in the out-of-central area.

Figure 7 (a-b) shows the pressure distribution along the airways, starting from throat to generation 5 for all age-specific cases at differing inlet conditions of 7.5 lpm and 15 lpm. It is obvious from this figure that the pressure value decreases in the lower airways compared to the upper airways. This pressure drop generates the airflow in human airways. According to Figure 7, the pressure value for 50-year-olds is lower than for 70 year-olds in all locations in the airways. The pressure value for 60-year-old subjects is higher than other subjects in areas from mouth-throat to generation 3. The pressure value in generation 5 of 60-year-old subjects is

lower than for other-aged subjects. When the inhalation rate is 7.5 lpm, the pressure drop between the mouth and generation 5 for 60-year-old subjects is about 6.5 Pa, while the pressure drops for the 50-year and 70-year old subjects are about 2 Pa and 3.5 Pa, respectively. Overall, it implies that the pressure drops as the human lung ages

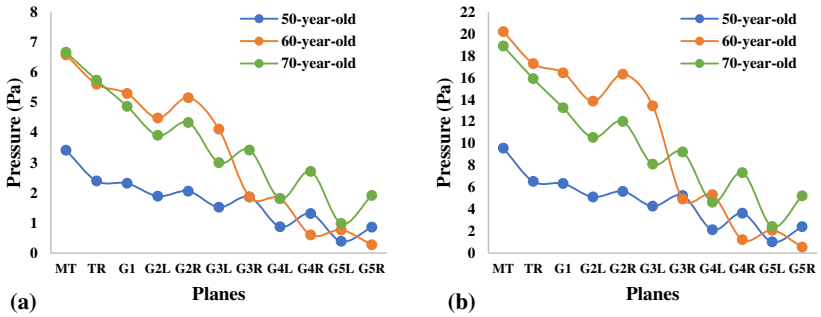

Figure 7. Pressure at various selected positions for three lung cases at **(a)** 7.5 lpm, and **(b)** 15 lpm. MT, mouth-throat; TR, trachea; G1, Generation 1; G2L, Generation 2-left lung; G2R, Generation 2-right lung; G3L, Generation 3-left lung; G3R, Generation 3-right lung; G4L, Generation 4-left lung; G4R, Generation 4-right lung; G5L, Generation 5-left lung; G5R, Generation 5-right lung.

The deposition of SARS Coronavirus-2 aerosol in the human upper and lower airways is representative of the transport behaviour of Covid-19 within the human airways. Figure 8 represents the deposition of different size SARS Coronavirus-2 aerosol at the mouth-throat area. Figure 9 (a) and Figure 9 (b) show the efficiency of SARS Coronavirus-2 aerosol deposition in the mouth area for various sizes under inhalation rates of 7.5 lpm and 15 lpm, respectively. According to Figure 9(a-b), in the mouth area, smaller SARS Coronavirus-2 aerosol deposition is greater than larger SARS Coronavirus-2 particles for all models. Figure 9 (a) shows at 7.5 lpm case, the DE of smaller SARS Coronavirus-2 aerosol (120 nm) in the mouth-throat area increases with aging; however, for a bigger SARS Coronavirus-2 aerosol (i.e., 500 nm) the DE of 60-year-old subjects is higher than for the other two 50- and 70-year-old subjects. This relationship between the DE and the age of the subject occurs for micro-size SARS Coronavirus-2 aerosols as well. The Brownian motion is the main mechanism for smaller diameter aerosol. The low inlet velocity, smaller diameter aerosol and highly assymetric airway model increase the deposition concentration at the mouth-throat section. In contrast, at 15 lpm, the DE of SARS Coronavirus-2 aerosol in the mouth-throat area for 60-year-old subjects is lower than for 50- and 70-year olds. Comparing Figure 9 (a) and Figure 9 (b), the DE of larger SARS Coronavirus-2 aerosol for 60-year old subjects is greater than 50- and 70- year-old subjects under both flow conditions. However, by increasing the age from 50 to 70, the DE of the larger SARS Coronavirus-2 aerosol (1 µm) decreases when the inhalation rate is 7.5 lpm, while it increases at the inhalation rate of 15 lpm.

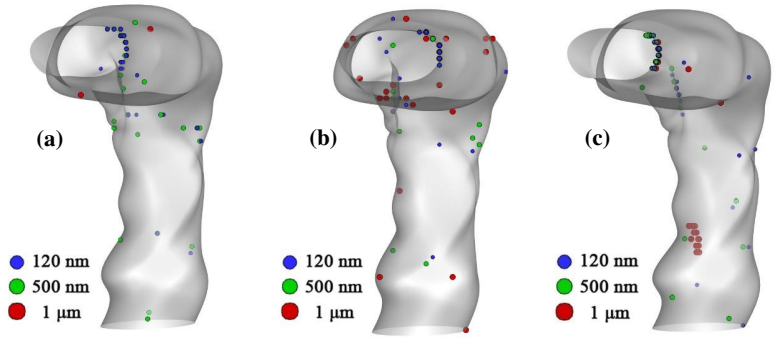

Figure 8. Deposition scenario at mouth-throat area at 15 lpm, **(a)** for 50-year-old subject, **(b)** for 60-year-old subject, and **(c)** for 70-year-old subject.

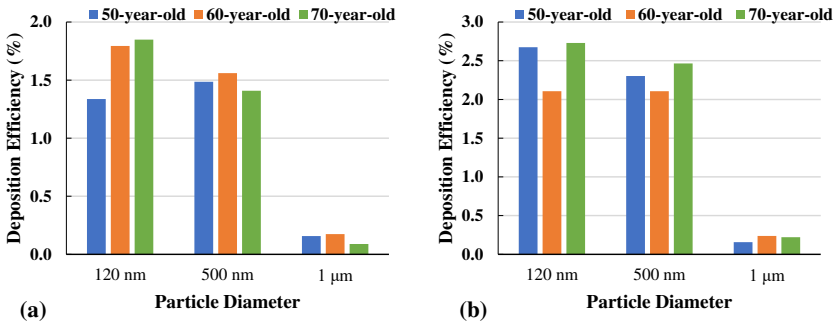

Figure 9. Particle DE comparison in the mouth-throat area for three lung models, **(a)** at 7.5 lpm, and **(b)** at 15 lpm.

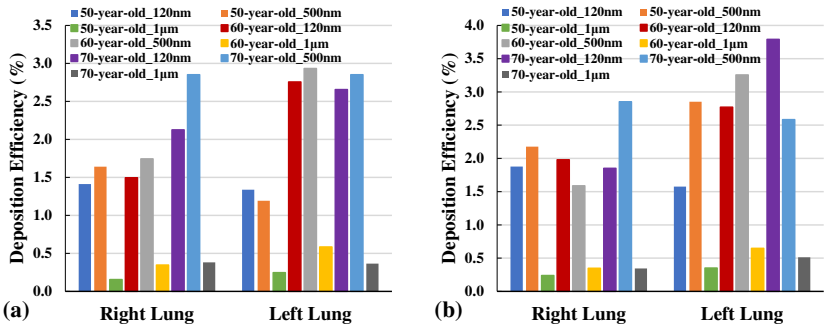

Figure10. SARS Coronavirus-2 Aerosol DE at right and left bronchioles, **(a)** for 7.5 lpm, and **(b)** for 15 lpm.

Figure 10 illustrates the SARS Coronavirus-2 Aerosol DE in the left and right lungs under different inlet flow rates. As can be seen from Figure 10 (a), the lowest DE for all cases occurs when the SARS Coronavirus-2aerosols are in microscale (i.e., 1 µm). When the flow rate is 7.5 lpm, the highest DE in the right lung corresponds to the 60-year-old subject with aerosol diameter of 500 nm. Also, the DE in the right lung for 500 nm SARS coronavirus-2 increases with the increasing age of the subjects. Figure 10 (a) also shows that when the inhalation rate is 7.5 lpm, the DE decreases considerably with increasing aerosol size for the youngest subjects (i.e., 50-year-olds). Figure 10 (b) demonstrates that the DE in the right lung decreases significantly with increasing particle size for 60-year-old subjects when the inhalation rate is 15 lpm. This behaviour between the aerosol particle size and DE can also be seen in the left lung for an older subject (70-year-old). According to Figure 10, the highest DE in the left lung occurs for the oldest subject i.e., 70-year-old under inlet condition of 15 lpm, with is about 3.5%. Figure 10 also demonstrates that the DE of the larger SARS Coronavirus-2 Aerosol (1 micron) in the right lung has an increasing trend with aging under both inhalation conditions.

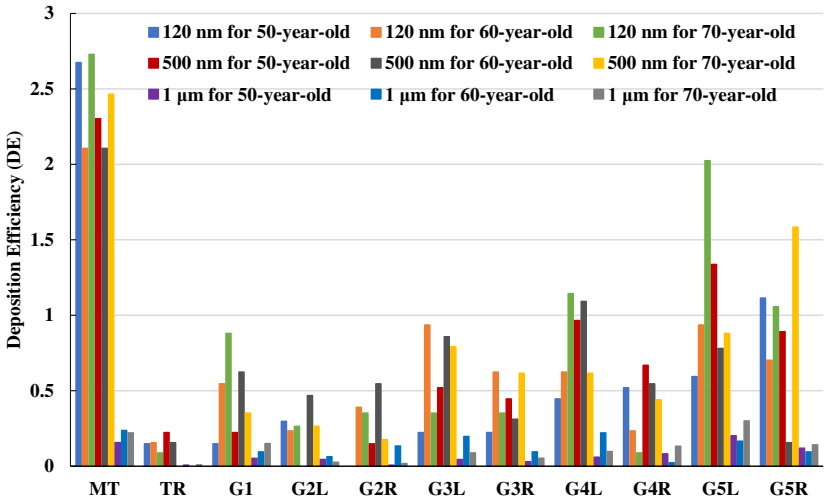

Figure 11. Depositions hot spot comparison for different diameters at 15lpmofinlet conditions.

Figure 11 presents the DEatdifferent locations from the mouth-throat region to the fifth generation of human airways for different particle size SARS Coronavirus-2 Aerosols and for various age-specific subjects for flows of 15 lpm. It is clear from this figure that the highest DE occurs in the mouth-throat region, while DE lowers in the tracheal region. The high deposition in the mouth-throat regions is due to this area's bending shape, which exerts a centrifugal force on the particles passing through the throat. The lower DE in the trachea occurs due to its cylindrical shape where no sudden change in the flow direction occurs. On the other hand, the DE increases along the airways from the trachea to the tracheobronchial airways of the lung. Among the generations, the downstream generation in this study, i.e. generation 5, has the highest DE, which is due to the fact that when generations progress toward the lung, the diameter of the airways decreases, and the majority of the particles come closer to the walls and the possibility of particle deposition increases. Figure 11 also shows that a decrease in particle diameter increases the local DE in generations 1, 4-left, and 5-left. Moreover, this figure demonstrates that the lowest generation of the left lung (i.e., generation 5) has the highest DE for the oldest subject with aerosol diameter of 120 nm.

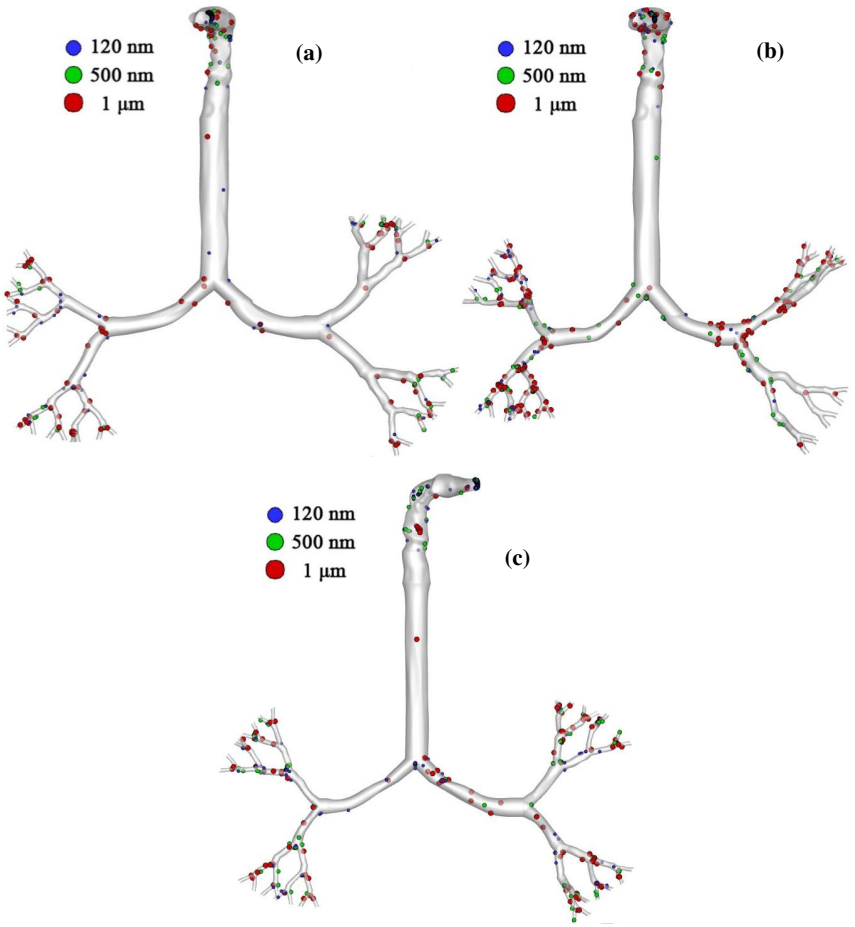

Figure 12. Particle deposition scenario at 15lpm flow rate for **(a)** 50-year-old, **(b)** 60-year-old, and **(c)** 70-year-old.

Figure 12 shows an overview of particle deposition in the whole geometry from mouth to fifth generation. From this Figure it can be seen that the SARS Coronavirus-2 aerosols are mostly deposited at the mouth-throat and bifurcation area of the upper airway models. The overall deposition scenario shows higher SARS Coronavirus-2 aerosol depositions for aged subjects than for the younger ones. The general deposition pattern shows smaller diameter SARS Coronavirus-2 aerosol particles are mostly deposited in the upper airways than are the larger sized SARS Coronavirus-2 aerosol particles. It is evident from the literature that Brownian motion is the principal mechanism of the smaller diameter (nano) particle transport in the human bronchial tree (Farhadi Ghalati *et al*., 2012; Ghosh *et al*., 2020; Zhang *et al.*, 2004). The Brownian motion will be more dominant when the inhalation rate is minimum and the random movement of the smaller diameter aerosol particles increases the deposition concentration in

the upper airways (Islam *et al*., 2017b). At low inlet conditions, smaller diameter aerosols randomly move inside the airways, and the spontaneous movement increases the deposition at the highly asymmetric mouth-throat and upper airways.

Conclusions

The SARS Coronavirus-2 aerosol depositions are numerically investigated for the first time for age-specific lungs. Three upper lung airway models for 50-, 60-, and 70-year-olds are developed, based on various SARS Coronavirus-2 aerosol particle sizes and flow rates. An inclusive analysis is performed for the airflow and pressure variations throughout the upper airways (generations 1 to 5). A comprehensive generation-by- generation SARS Coronavirus-2 aerosol DE is calculated and presented. Some key findings of the study are summarized below;

- The general pressure variation from mouth-throat to 5th generation of the upper airway model increases with age. At 7.5 lpm case, the highest pressure is observed for 70-year old lungs, while lowest pressure is observed for 50-year old lungs. On the contrary, the 15 lpm inhalation case results indicate the highest pulmonary pressure occurs for the 60-year old model.
- The SARS Coronavirus-2 aerosol DE for smaller diameter SARS Coronavirus-2 aerosols is higher than the larger diameter SARS Coronavirus-2 aerosols, irrespective of the inhalation conditions.
- The overall DE of the SARS Coronavirus-2 aerosols for aged lungs is found higher than for the younger counterparts. Almost all cases (irrespective of flow conditions and aerosol particle sizes) show higher depositions for 70-year old lungs than for 50-year and 60-year old counterparts.
- The SARS Coronavirus-2 aerosols demonstrate a highly complex deposition pattern in the right and the left lung respectively. At a 7.5 lpm flow rate, smaller diameter SARS Coronavirus-2 aerosol particle deposition in the right lung is greater than in the left lung. On the contrary, larger diameter SARS Coronavirus-2 aerosol particle deposition is higher in the left lung than in the left lung. A similar trend is observed for 15 lpm inhalation conditions for various particle diameters of SARS Coronavirus-2 aerosols.
- The SARS Coronavirus-2 aerosol shows high concentration at the mouth-throat region for all deposition parameters than in the bifurcating branches. The aerosol deposition concentration is also found to be higher at the fifth generations of the left and the right lungs.
- The overall DE of the SARS Coronavirus-2 aerosol increases from upper generations to lower generations (i.e. from generation 1 to 5).

In this study the SARS Coronavirus-2 deposition at the mouth-throat and upper airways of the age-specific lung was critically analysed and led to the identification of a high-concentration deposition zone. In the study a range of SARS Coronavirus-2 aerosol diameter was considered. The specific findings of this study would improve the knowledge of the SARS Coronavirus-2 aerosol transport to the upper airways of the age-specific lung. The comprehensive generation by generation deposition data for age-specific lung could be useful for the health risk assessment of the SARS Coronavirus-2 affected aged people.

Conflicts of the Interest

No conflicts of interest are reported.

Acknowledgement:

The authors thank the UTS iHPC support and UTS ECR Development Initiative Grant PR019-8377. The author Y.T. Gu thanks support from the Australian Research Council (ARC) grants DP180103009 and IC190100020.

Data Availability:

The data could be available from the corresponding author upon reasonable request.

References

Al-Zahrani, J. SARS-CoV-2 associated COVID-19 in geriatric population: A brief narrative review. Saudi Journal of Biological Sciences, volume 28, issue 1, 2021, pp. 738-743, https://doi.org/10.1016/j.sjbs.2020.11.001.

Ayoub HH, Chemaitelly H, Seedat S, Mumtaz GR, Makhoul M, Abu-Raddad LJ (2020). Age could be driving variable SARS-CoV-2 epidemic trajectories worldwide. PLoS ONE 15(8): e0237959. https://doi.org/10.1371/journal.pone.0237959

Bai, T.R., Cooper, J., Koelmeyer, T., Paré, P.D. and Weir, T.D., 2000. The Effect of Age and Duration of Disease on Airway Structure in Fatal Asthma. Am J Respir Crit Care Med. 162: 663–669.

Bass, K., Thomas, M.L., Kemner-van de Corput, M.P., Tiddens, H.A., Longest, P.W., 2021. Development of Characteristic Airway Bifurcations in Cystic Fibrosis. J Aerosol Science Technology, 1-26.

Bhattacharyya, S., Dey, K., Paul, A.R. and Biswas, R. 2020. A Novel CFD Analysis to Minimize the Spread of COVID-19 Virus in Hospital Isolation Room. Chaos, Solitons & Fractals, 139:110294. DOI: 10.1016/j.chaos.2020.110294

Chen, W.-H., Chang, C.-M., Mutuku, J.K., Lam, S.S., Lee, W.-J., 2021. Aerosol deposition and airflow dynamics in healthy and asthmatic human airways during inhalation. J Journal of Hazardous Materials 416, 125856.

Cheng, K.-H., Cheng, Y.-S., Yeh, H.-C., Swift, D.L., 1995a. Deposition of ultrafine aerosols in the head airways during natural breathing and during simulated breath holding using replicate human upper airway casts. J Aerosol ScienceTechnology 23, 465-474.

Cheng, K.-H., Swift, D.L., technology, 1995b. Calculation of total deposition fraction of ultrafine aerosols in human extrathoracic and intrathoracic regions. J Aerosol science 22, 194-201.

Chirizzi, D., Conte, M., Feltracco, M., Dinoi, A., Gregoris, E., Barbaro, E., La Bella, G., Ciccarese, G., La Salandra, G., Gambaro, A., 2021. SARS-CoV-2 concentrations and virus-laden aerosol size distributions in outdoor air in north and south of Italy. J Environment International 146, 106255.

Clarfield, A.M., Jotkowitz, A. Age, ageing, ageism and "age-itation" in the Age of COVID-19: rights and obligations relating to older persons in Israel as observed through the lens of medical ethics. Isr J Health Policy Res 9, 64 (2020). https://doi.org/10.1186/s13584-020-00416-y

Cui, X., Ge, H., Wu, W., Feng, Y., Wang, J., 2021. LES study of the respiratory airflow field in a whole-lung airway model considering steady respiration. J Journal of the Brazilian Society of Mechanical Sciences Engineering 43, 1-17.

Das P, Nof E, Amirav I, Kassinos SC, Sznitman J (2018) Targeting inhaled aerosol delivery to upper airways in children: Insight from computational fluid dynamics (CFD). PLoS ONE 13 (11): e0207711. https://doi.org/10.1371/journal.pone.0207711

Davies, N.G., Klepac, P., Liu, Y. et al. Age-dependent effects in the transmission and control of COVID-19 epidemics. Nat Med 26, 1205–1211 (2020). https://doi.org/10.1038/s41591-020-0962-9

Edwards, D.A., Ausiello, d., Salzman, J., Devlin, T., Langer, R., Beddingfield, B.J., Fears, A.C., Doyle-Meyers, L.A., Redmann, R.K., Killeen, S.Z., Maness, N.J. and Roy, C.J.. 2021. Exhaled aerosol increases with COVID-19 infection, age, and obesity. PNAS. 118 (8) e2021830118; https://doi.org/10.1073/pnas.2021830118

Fan, Z., Holmes, D., Sauret, E., Islam, M.S., Saha, S.C., Ristovski, Z., Gu, Y.T., 2021. A multiscale modelling method incorporating spatial coupling and temporal coupling into transient simulations of the human airways. J International Journal for Numerical Methods in Fluids.

Farhadi Ghalati, P., Keshavarzian, E., Abouali, O., Faramarzi, A., Tu, J., Shakibafard, A., 2012. Numerical analysis of micro- and nano-particle deposition in a realistic human upper airway. Comput Biol Med 42, 39-49.

Gemci, T., Ponyavin, V., Chen, Y., Chen, H., Collins, R., 2008. Computational model of airflow in upper 17 generations of human respiratory tract. Journal of Biomechanics 41, 2047-2054.

Ghosh, A., Islam, M.S., Saha, S.C., 2020. Targeted drug delivery of magnetic nano-particle in the specific lung region. J Computation 8, 10.

Goldsmith, C.S., Miller, S.E., Martines, R.B., Bullock, H.A., Zaki, S.R., 2020. Electron microscopy of SARS-CoV-2: a challenging task. J The Lancet 395, e99.

Guo T, Shen Q, Guo W, He W, Li J, Zhang Y, Wang Y, Zhou Z, Deng D, Ouyang X, Xiang Z, Jiang M, Liang M, Huang P, Peng Z, Xiang X, Liu W, Luo H, Chen P, Peng H: Clinical Characteristics of Elderly Patients with COVID-19 in Hunan Province, China: A Multicenter, Retrospective Study. Gerontology 2020; 66:467-475. doi: 10.1159/000508734

Guzman, M.I. 2021. An overview of the effect of bioaerosol size in coronavirus disease 2019 transmission. The International J. of health Planning and Management, 36 (2): 257-266. https://doi.org/10.1002/hpm.3095.

Haider, A., Levenspiel, O.J.P.t., 1989. Drag coefficient and terminal velocity of spherical and nonspherical particles. J Powder technology 58, 63-70.

Hayati, H., Feng, Y., Hinsdale, M., 2021. Inter-species variabilities of droplet transport, size change, and deposition in human and rat respiratory systems: An in silico study. J Journal of Aerosol Science 154, 105761.

Holt, NR; Neumann, JT; McNeil, JJ; Cheng, AC. Implications of COVID-19 for an ageing population. The Medical Journal of Australia, volume 213, issue 8, 2020, pp. 342-344. https://doi.org/10.5694/mja2.50785

https://www.nih.gov/news-events/nih-research-matters/novel-coronavirus-structure-reveals-targets-vaccines-treatment

https://www.pptaglobal.org/media-and-information/ppta-statements/1055-2019-novel-coronavirus-2019-ncov-and-plasma-protein-therapies.

Inthavong, K., Tu, J., Ahmadi, G., 2009. Computational modelling of gas-particle flows with different particle morphology in the human nasal cavity. The Journal of Computational Multiphase Flows 1, 57-82.

Islam, M.S., Larpruenrudee, P., Hossain, S.I., Rahimi-Gorji, M., Gu, Y., Saha, S.C., Paul, G., 2021a. Polydisperse Aerosol Transport and Deposition in Upper Airways of Age-Specific Lung. J International Journal of Environmental Research Public Health 18, 6239.

Islam, M.S., Larpruenrudee, P., Hossain, S.I., Rahimi-Gorji, M., Gu, Y., Saha, S.C., Paul, G., Health, P., 2021b. Polydisperse Aerosol Transport and Deposition in Upper Airways of Age-Specific Lung. J International Journal of Environmental Research 18, 6239.

Islam, M.S., Larpruenrudee, P., Paul, A.R., Paul, G., Gemci, T., Gu, Y., Saha, S.C., 2021c. SARS Coronavirus-2 aerosol: How far it can travel to the lower airways? J Physics of Fluids 33, 061903.

Islam, M.S., S. C. Saha, E. Sauret, T. Gemci, Y. T. Gu, 2017. Pulmonary aerosol transport and deposition analysis in upper 17 generations of the human respiratory tract. Journal of Aerosol Science 108: 29-43.

Islam, M.S., Saha, S.C., Gemci, T., Yang, I.A., Sauret, E., Gu, Y.T., 2018. Polydisperse Microparticle Transport and Deposition to the Terminal Bronchioles in a Heterogeneous Vasculature Tree. Scientific Reports 8, 16387.

Islam, M.S., Saha, S.C., Gemci, T., Yang, I.A., Sauret, E., Ristovski, Z., Gu, Y.T., 2019. Euler-Lagrange Prediction of Diesel-Exhaust Polydisperse Particle Transport and Deposition in Lung: Anatomy and Turbulence Effects. Scientific Reports 9, 12423.

Islam, M.S., Saha, S.C., Sauret, E., Gemci, T., Gu, Y., 2017a. Pulmonary aerosol transport and deposition analysis in upper 17 generations of the human respiratory tract. Journal of Aerosol Science 108, 29-43.

Islam, M.S., Saha, S.C., Sauret, E., Gemci, T., Yang, I.A., Gu, Y., 2017b. Ultrafine particle transport and deposition in a large scale 17-generation lung model. Journal of biomechanics 64, 16-25.

Islam, M.S.; Paul, G.; Ong, H.X.; Young, P.M.; Gu, Y.T.; Saha, S.C. A Review of Respiratory Anatomical Development, Air Flow Characterization and Particle Deposition. Int. J. Environ. Res. Public Health 2020, 17, 380. https://doi.org/10.3390/ijerph17020380

Jaafar-Maalej, C., Andrieu, V., Elaissari, A. and Fessi, H. (2009) Assessment methods of inhaled aerosols: technical aspects and applications, Expert Opinion on Drug Delivery, 6:9, 941-959, DOI: 10.1517/17425240903117244

Jarvis M.C. (2020) Aerosol Transmission of SARS-CoV-2: Physical Principles and Implications. Front. Public Health 8:590041. doi: 10.3389/fpubh.2020.590041

Kelly, J.T., Asgharian, B., Kimbell, J.S., Wong, B.A., 2004. Particle deposition in human nasal airway replicas manufactured by different methods. Part II: Ultrafine particles. J Aerosol science Technology 38, 1072-1079.

Kim J, Heise RL, Reynolds AM, Pidaparti RM (2017) Aging effects on airflow dynamics and lung function in human bronchioles. PLoS ONE 12(8): e0183654. https://doi.org/10.1371/journal.pone.0183654

Kim, J., O'Neill, J.D., Dorrello, N.V., Bacchetta, M., Vunjak-Novakovic, G. 2015. Targeted delivery of liquid microvolumes into lung. Proceedings of the National Academy of Sciences, 112 (37) 11530-11535; DOI: 10.1073/pnas.1512613112

Kleinstreuer, C., Zhang, Z.J.I.J.o.M.F., 2003. Laminar-to-turbulent fluid-particle flows in a human airway model. 29, 271-289.

Knudson R.J.: Physiology of the aging lung. In: Crystal R.G., West J.B. (Eds.), The lung scientific foundations. Raven Press, New York, 1991, pp. 1749-1759.

Koff WC, Williams MA. Covid-19 and Immunity in Aging Populations - A New Research Agenda. N Engl J Med. 2020 Aug 27;383(9):804-805. doi: 10.1056/NEJMp2006761. Epub 2020 Apr 17. PMID: 32302079.

Kumar, B., Srivastav, V.K., Jain, A. and Paul, A.R. 2019. Study of Numerical Schemes for the CFD Simulation of Human Airways. International Journal of Integrated Engineering. 11(8): 32-40.

Kuprat, A.P., Jalali, M., Jan, T., Corley, R.A., Asgharian, B., Price, O., Singh, R.K., Colby, S., Darquenne, C., 2021. Efficient bi-directional coupling of 3D computational fluid-particle dynamics and 1D Multiple Path Particle Dosimetry lung models for multiscale modeling of aerosol dosimetry. J Journal of Aerosol Science 151, 105647.

Labiris, N.R. and Dolovich, M.B., 2003. Pulmonary drug delivery. Part I: Physiological factors affecting therapeutic effectiveness of aerosolized medications. British Journal of Clinical Pharmacology, vol. 56, issue 6, pp. 588-599. https://doi.org/10.1046/j.1365-2125.2003.01892.x

Lai-Fook SJ, Hyatt RE. Effects of age on elastic moduli of human lungs. Journal of applied physiology. 2000; 89(1):163±8. PMID: 10904048

Leblanc P., Ruff F., Milic-Emili J.: Effects of age and body position on "airway closure" in man. J. Appl. Physiol. 28: 448-451, 1970.

Liu K, Chen Y, Lin R, Han K. Clinical features of COVID-19 in elderly patients: a comparison with young and middle-aged patients. J Infect. (2020a) 80:e14–8. doi: 10.1016/j.jinf.2020.03.005

Liu, Y., Ning, Z., Chen, Y., Guo, M., Liu, Y., Gali, N.K., Sun, L., Duan, Y., Cai, J., Westerdahl, D., 2020b. Aerodynamic analysis of SARS-CoV-2 in two Wuhan hospitals. J Nature 582, 557-560.

Lowery EM, Brubaker AL, Kuhlmann E, Kovacs EJ. The Aging Lung. Clin Interv Aging 2013;8:1489–96.

Mallik, A.K., Mukherjee, S. and Panchagnula, M.V. 2020. An experimental study of respiratory aerosol transport in phantom lung bronchioles. Phys. Fluids 32, 111903; https://doi.org/10.1063/5.0029899

Miller EJ, Linge HM. Age-related changes in immunological and physiological responses following pulmonary challenge. Int J Mol Sci. (2017) 18:1294. doi: 10.3390/ijms18061294

Montaudon M, Desbarats P, Berger P, De Dietrich G, Marthan R, Laurent F. Assessment of bronchial wall thickness and lumen diameter in human adults using multi-detector computed tomography: comparison with theoretical models. Journal of anatomy. 2007; 211(5):579±88. https://doi.org/10.1111/j.1469-7580.2007.00811.x PMID: 17919291

Mueller AL, McNamara MS, Sinclair DA. Why does COVID-19 disproportionately affect older people? Aging (Albany NY). 2020 May 29;12(10):9959-9981. doi: 10.18632/aging.103344. Epub 2020 May 29. PMID: 32470948; PMCID: PMC7288963.

Mutuku, J.K., Hou, W.C. and Chen, W.H. (2020). An Overview of Experiments and Numerical Simulations on Airflow and Aerosols Deposition in Human Airways and the Role of Bioaerosol Motion in COVID-19 Transmission. Aerosol Air Qual. Res. 20: 1172–1196. https://doi.org/10.4209/aaqr.2020.04.0185

Niewoehner D.E., Kleinerman J.: Morphologic basis of pulmonary resistance in the human lung and effects of aging. J. Appl. Physiol. 36: 412-418, 1974.

Ostrovski Y, Dorfman S, Mezhericher M, Kassinos S, Sznitman J. Targeted Drug Delivery to Upper Airways Using a Pulsed Aerosol Bolus and Inhaled Volume Tracking Method. Flow Turbul Combust. 2019 Jan;102(1):73-87. doi: 10.1007/s10494-018-9927-1. Epub 2018 May 2. PMID: 30956537; PMCID: PMC6445363.

Perrotta, F., Corbi, G., Mazzeo, G. et al. COVID-19 and the elderly: insights into pathogenesis and clinical decision-making. Aging Clin Exp Res 32, 1599–1608 (2020). https://doi.org/10.1007/s40520-020-01631-y

Pride, N.B. Ageing and changes in lung mechanics. Eur Respir J 2005; 26(4): 563–565. DOI: 10.1183/09031936.05.00079805

Rossi, A., Ganassini, A., Tantucci, C. and Grassi, V. Aging and the respiratory system. Aging Clin. Exp. Res. 8: 143-161, 1996.

Sandoiu, A., The impact of the COVID-19 pandemic on older adults, published in Medical News Today, retreived on 7 April 2021. https://www.medicalnewstoday.com/articles/the-impact-of-the-covid-19-pandemic-on-older-adults

Santesmasses, D; Castro, JP; Zenin, AA; Shindyapina, AV; Gerashchenko, MV; Zhang, B; Kerepesi, C; Yim, SH; Fedichev, PO; Gladyshev, VN. COVID-19 is an emergent disease of aging. medRxiv

2020.04.15.20060095; doi: https://doi.org/10.1101/2020.04.15.20060095

Sharma, G., Goodwin, J. Effect of aging on respiratory system physiology and immunology. Clinical Interventions in Aging 2006:1(3) 253–260

Shukla, R.K., Srivastav, V.K., Paul, A.R. and Jain, A. 2020. Fluid Structure Interaction Studies of Human Airways", Sādhanā Journal. 45(229): 1-6. https://doi.org/10.1007/s12046-020-01460-9

Singh D., Jain A. and Paul A.R., 2021. Numerical Study on Particle Deposition in Healthy Human Airways and Airways with Glomus Tumor. In: Rizvanov A.A., Singh B.K., Ganasala P. (eds) Advances in Biomedical Engineering and Technology. Lecture Notes in Bioengineering. Springer, Singapore. https://doi.org/10.1007/978-981-15-6329-4_31

Singh HP, Khullar V, Sharma M. Estimating the Impact of Covid-19 Outbreak on High-Risk Age Group Population in India. Augmented Human Research. 2020; 5(1):18. doi:10.1007/s41133-020-00037-9

Smorenberg, A. Peters, E JG, van Daele, P LA, Nossent, EJ, Muller, M. How does SARS-CoV-2 targets the elderly patients? A review on potential mechanisms increasing disease severity. European Journal of Internal Medicine, volume 83, 2021, pp. 1-5, https://doi.org/10.1016/j.ejim.2020.11.024

Srivastav, V. K., A. R. Paul, A. Jain, 2013. Effects of cartilaginous rings on airflow and particle transport through simplified and realistic models of human upper respiratory tracts, Acta Mechanica Sinica 29(6): 883–892. doi: 10.1007/s10409-013-0086-2

Srivastav, V.K., A. Kumar, S. K. Shukla, A. R. Paul, A. D. Bhatt, A. Jain, 2014. Airflow and aerosol-drug delivery in a CT scan based human respiratory tract with tumor using CFD, Journal of Applied Fluid Mechanics 7(2): 345-356.

Srivastav, V.K., Jain, A. and Paul, A.R., 2019a. Computational Study of Drug Delivery in Tumorous Human Airways. International Journal of Computing Science and Mathematics. 10(5): 459-475. https://doi.org/10.1504/IJCSM.2019.103676

Srivastav, V.K., Paul, A.R. and Jain, A., 2019b. Capturing the Wall Turbulence in CFD Simulation of Human Respiratory Tract. Mathematics and Computers in Simulation. 160:23-38. https://doi.org/10.1016/j.matcom.2018.11.019

Srivastav, V.K., Jain, A., Paul, A.R., 2021. Computational Studies of Aerosolized Drug Deposition in Human Respiratory Tract, Chapter 2, pp. 1-10, In: Lecture Notes in Mechanical Engineering, L. Venkatakrishnan et al. (Eds.): Proceedings of 16th Asian Congress of Fluid Mechanics, Online ISBN: 978-981-15-5183-3, Hardcover ISBN: 978-981-15-5182-6, No. of pages: XVII, 373, Publisher: Springer, Singapore. https://doi.org/ 10.1007/978-981-15-5183-3_2

Stocks, J. Quanjer, Ph.H., Reference values for residual volume, functional residual capacity and total lung capacity. Eur Respir J, 1995, 8, 492–506 DOI: 10.1183/09031936.95.08030492

Swift, D.L., Montassier, N., Hopke, P.K., Karpen-Hayes, K., Cheng, Y.-S., Su, Y.F., Yeh, H.C., Strong, J.C., 1992. Inspiratory deposition of ultrafine particles in human nasal replicate cast. J Journal of aerosol science 23, 65-72.

Tang, S., Mao, Y., Jones, R.M., Tan, Q., Ji, J.S., Li, N., Shen, J., Lv, Y., Pan, L., Ding, P., Wang, X., Wang, Y., MacIntyre, C.R., Shi, X. 2020. Aerosol transmission of SARS-CoV-2? Evidence, prevention and control, Environment International. 144: 106039, https://doi.org/10.1016/j.envint.2020.106039

Thompson, P.J., 1998. Drug Delivery to the Small Airways. American Journal of Respiratory and Critical Care Medicine, vol. 157, issue 5, pp. 199-202. https://doi.org/10.1164/ajrccm.157.5.rsaa-7

Tiwari, A., Sharma, S., Srivastav, V.K., Jain, A. and Paul, A.R., 2021. Computational Study of Atomization Models and Optimal Design of a Pressurized Inhaler. Journal of Biomimetics, Biomaterials and Biomedical Engineering. 50: 124-135. https://doi.org/10.4028/www.scientific.net/JBBBE.50.123

Xu, G. and C. Yu, 1986. Effects of age on deposition of inhaled aerosols in the human lung. Aerosol Science and Technology. 5(3): p. 349-357.

Zhang, Z., Kleinstreuer, C., 2004. Airflow structures and nano-particle deposition in a human upper airway model. Journal of computational physics. 198, 178-210.

Zhang, Z., Kleinstreuer, C., 2011. Computational analysis of airflow and nanoparticle deposition in a combined nasal–oral–tracheobronchial airway model. J Journal of Aerosol Science 42, 174-194.

Zhang, Z., Kleinstreuer, C., Donohue, J.F., Kim, C.S., 2005. Comparison of micro- and nano-size particle depositions in a human upper airway model. Journal of Aerosol Science 36, 211-233.

Zhao, J., Feng, Y., Tian, G., Taylor, C., Arden, N.S., 2021. Influences of puff protocols and upper airway anatomy on cannabis pharmacokinetics: A CFPD-PK study. J Computers in biology medicine 132, 104333.

Zhu N, Zhang D, Wang W, Li X, Yang B, Song J, Zhao X, Huang B, Shi W, Lu R, Niu P, Zhan F, Ma

Weibel, E. R., Cournand, A. F., & Richards, D. W. (1963). *Morphometry of the human lung* (Vol. 1). Berlin: Springer.
X, Wang D, Xu W, Wu G, Gao GF, Tan W; China Novel Coronavirus Investigating and Research Team. A Novel Coronavirus from Patients with Pneumonia in China, 2019. N Engl J Med. 2020 Feb 20;382(8):727-733. doi: 10.1056/NEJMoa2001017. Epub 2020 Jan 24. PMID: 31978945; PMCID: PMC7092803

Talib Dbouk and Dimitris Drikakis , "On airborne virus transmission in elevators and confined spaces", Physics of Fluids 33, 011905 (2021) https://doi.org/10.1063/5.0038180

Zhaobin Li, Xinlei Zhang, Ting Wu, Lixing Zhu, Jianhua Qin, and Xiaolei Yang, "Effects of slope and speed of escalator on the dispersion of cough-generated droplets from a passenger", Physics of Fluids 33, 041701 (2021a) https://doi.org/10.1063/5.0046870

Xiujie Li, Cheuk Ming Mak, Kuen Wai Ma, and Hai Ming Wong , "Evaluating flow-field and expelled droplets in the mockup dental clinic during the COVID-19 pandemic", Physics of Fluids 33, 047111 (2021b) https://doi.org/10.1063/5.0048848

Ata Nazari, Moharram Jafari, Naser Rezaei, Farzad Taghizadeh-Hesary, and Farhad Taghizadeh-Hesary , "Jet fans in the underground car parking areas and virus transmission", Physics of Fluids 33, 013603 (2021) https://doi.org/10.1063/5.0033557

Zhihang Zhang, Taehoon Han, Kwang Hee Yoo, Jesse Capecelatro, André L. Boehman, and Kevin Maki , "Disease transmission through expiratory aerosols on an urban bus", Physics of Fluids 33, 015116 (2021) https://doi.org/10.1063/5.0037452

Khaled Talaat, Mohamed Abuhegazy, Omar A. Mahfoze, Osman Anderoglu, and Svetlana V. Poroseva , "Simulation of aerosol transmission on a Boeing 737 airplane with intervention measures for COVID-19 mitigation", Physics of Fluids 33, 033312 (2021) https://doi.org/10.1063/5.0044720

Aaron Foster and Michael Kinzel , "Estimating COVID-19 exposure in a classroom setting: A comparison between mathematical and numerical models", Physics of Fluids 33, 021904 (2021) https://doi.org/10.1063/5.0040755

Han Liu, Sida He, Lian Shen, and Jiarong Hong, "Simulation-based study of COVID-19 outbreak associated with air-conditioning in a restaurant", Physics of Fluids 33, 023301 (2021) https://doi.org/10.1063/5.0040188

Liangyu Wu, Xiangdong Liu, Feng Yao, and Yongping Chen, "Numerical study of virus transmission through droplets from sneezing in a cafeteria", Physics of Fluids 33, 023311 (2021) https://doi.org/10.1063/5.0040803

Dnyanesh Mirikar, Silambarasan Palanivel, and Venugopal Arumuru , "Droplet fate, efficacy of face mask, and transmission of virus-laden droplets inside a conference room", Physics of Fluids 33, 065108 (2021) https://doi.org/10.1063/5.0054110

Ruichen He, Wanjiao Liu, John Elson, Rainer Vogt, Clay Maranville, and Jiarong Hong, "Airborne transmission of COVID-19 and mitigation using box fan air cleaners in a poorly ventilated classroom", Physics of Fluids 33, 057107 (2021) https://doi.org/10.1063/5.0050058

Jesse H. Schreck, Masoud Jahandar Lashaki, Javad Hashemi, Manhar Dhanak, and Siddhartha Verma , "Aerosol generation in public restrooms", Physics of Fluids 33, 033320 (2021) https://doi.org/10.1063/5.0040310

Jie Zheng, Xiaofei Wu, Fangxin Fang, Jinxi Li, Zifa Wang, Hang Xiao, Jiang Zhu, Christopher Pain, Paul Linden, and Boyu Xiang , "Numerical study of COVID-19 spatial–temporal spreading in London", Physics of Fluids 33, 046605 (2021) https://doi.org/10.1063/5.0048472

Keiko Ishii, Yoshiko Ohno, Maiko Oikawa, and Noriko Onishi , "Relationship between human exhalation diffusion and posture in face-to-face scenario with utterance", Physics of Fluids 33, 027101 (2021) https://doi.org/10.1063/5.0038380

Paul, A.R.; Khan, F.; Jain, A.; Saha, S.C. Deposition of Smoke Particles in Human Airways with Realistic Waveform. *Atmosphere* 2021, *12*, 912. https://doi.org/10.3390/atmos12070912